# AN ANALYSIS OF GLIDER DATA AS AN INPUT TO A SONAR RANGE DEPENDENT ACOUSTIC PERFORMANCE PREDICTION MODEL

**Janice Sendt**

**Thales Underwater Systems, Thales Australia, 274 Victoria Road, Rydalmere NSW 2116 Australia**

**Janice.sendt@thalesgroup.com.au**

This paper describes an initial assessment of the role of glider data as an input into a sonar nowcast acoustic detection range prediction model. It includes an analysis of the temporal and spatial variability of the water column data measured by a glider in shallow Australian waters. The area covered by the data includes a region where there is a known persistent frontal feature. The glider data verified that a persistent front was present in the data.

## INTRODUCTION

One of the difficulties in underwater nowcast predictions for sonar acoustic detection ranges has often been the paucity of available water column data which can also have a very inhomogeneous distribution in both space and time. Ideally the acoustic calculation should consist of at least one or a number of sound velocity profiles (SVPs) across the required distance which gives a true representation of the variation in sound. Historically, the measured sound speed at a given location has either been calculated from measured temperature and salinity profiles or directly measured with a speed of sound sensor. Depending on the gradient within the SVP, sound may propagated well in the water column or be dissipated at either of the boundaries.

A number of papers compare calculated transmission loss with at sea measurements in Australian waters [1,2]. The collecting of the necessary data within the time scale required for these calculations has been an expensive logistic exercise requiring support equipment in the form of aircraft or support vessels collecting SVPs across the required range and bearing/s.

For an operational system it has not been practical to expect access to this level of data collection on a regular ongoing basis, instead for nowcast sonar range predictions it has been the practice to use an insitu bathy drop (this contains a temperature probe which measures the profile and is supplemented with climatology data to characterise the water column). This situation changed about four years ago with the increasing availability of 3D gridded water column oceanographic data sets produced on an hourly basis [3].

An obvious source of water column data which has recently become available is from autonomous gliders. These have the ability to measure the water column ahead of a vessel, albeit slowly and to provide this data in a reasonably short time period. In addition, there can be multiple gliders concurrently collecting data so that many bearings can be covered simultaneously.

Autonomous gliders follow an up and down sawtooth profile through the water column sampling the water column for temperature and salinity approximately every 5 seconds. As the glider is driven by variable buoyancy it travels at approximately 1 km/hour (see Figure 1).

### Initial data assessment

The data was collected by Defence Science and Technology Organisation (DSTO) using two Slocum gliders over five days from 11th - 15th July 2011 at the top end of the Capricorn channel in the southern Great Barrier Reef area [4]. Figure 2 plots the route of the two gliders, named, glider “k85” which traversed further from the coast than glider “k90”. Cape Clinton is the nearest coastal feature spanning from 22.55°S to 22.65°S. The CTD probe fitted to the glider is Sea-Bird 41CP.

The Temperature-Salinity (T-S) diagram of all the data points for both gliders is shown in Figure 3. The features displayed in these plots differ due to the different glider routes with glider k85 traversing deeper water than glider k90. The maximum temperature was recorded by the k85 which was slightly less than 21°C compared to glider k90 which recorded a maximum temperature 0.05°C lower. The salinity range is greater for k85 than k90.

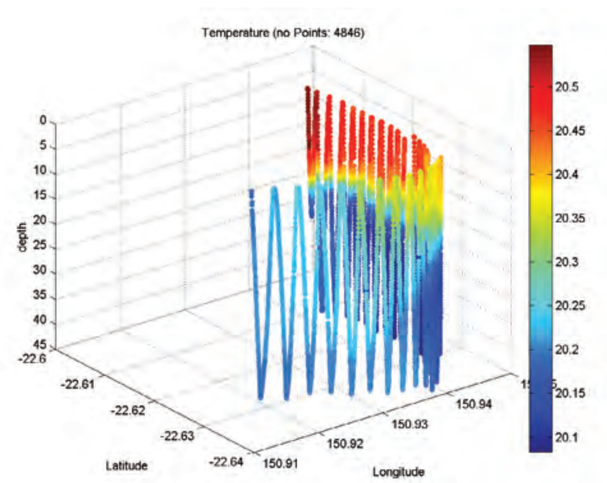


Figure 1. Raw temperature glider data showing the sawtooth profiles as a function of depth. Temperature measured in degrees Celsius and depth in metres

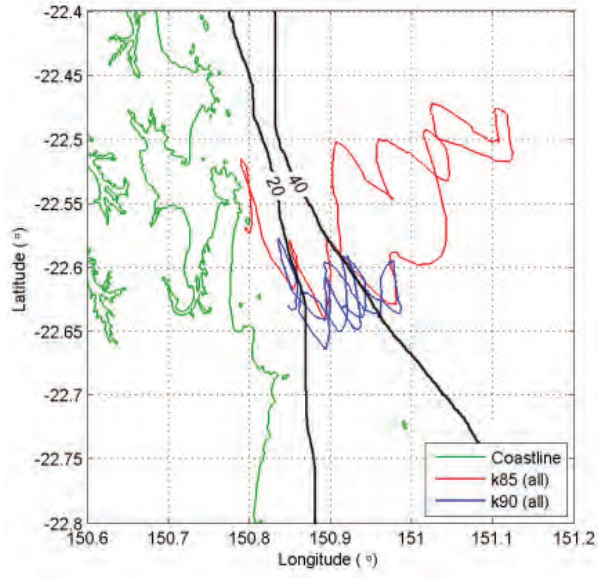


Figure 2. Route taken by the two gliders over a three day period starting late 11th July 2011. Depth contours are in metres

There are obvious differences in the features between the two glider T-S plots which could be due to the time of measurement and/or the location. When the glider data was reviewed in hourly time increments it became apparent that a parcel of cold water was traversed by glider k90 on the early morning of the 15th July. The maximum surface temperature was then reduced by 0.8°C in a 2 hour time period (see Figure 4). The second glider traversed the same area 8 hours later and the temperature profile exhibited similar changes symptomatic of a sustained front. For the salinity profile, there is a delay of some two hours after the temperature reaches its lowest value at 11 hours transit when the salinity values which have initially increased, then stabilise to a small range of values between surface and maximum glider depth. This is indicative of a well mixed water column. Thus the complexity of the two temperature/ salinity curves shown in Figure 3 is partially due to the overlaying of two parcels of water, one with a maximum temperature slightly below 21°C and the second with a maximum temperature at approximately 19.7°C.

**Ocean Currents**

Previous studies conducted in the area of the Southern Great Barrier Reef based on satellite thermal imaging have concluded that there is a persistent frontal feature, called the Clinton Cape front, caused by the impact of the change in coastal orientation on a northward moving, well-developed boundary current [5]. This front was described as a mushroom shaped jet of cold water starting from the coast, and extending eastward 245 km. Along the coast line the width of the root was 85 km and tapered at the throat to 18 km before expanding at the head to 105 km. An earlier reference found that the front was smaller, extending out 100 km [6]. The jet temperature was generally 1° to 2°C cooler than the surrounding water. It is hypothesised that the routes of both gliders crossed this frontal boundary. As there is no open source high resolution satellite sea surface temperature (SST) imagery for this time and area this cannot be independently verified. It is also assumed that waters within the jet are well mixed based on the T-S diagrams.

The boundary delineation where the temperature values become constant for the entire water column depth can be estimated by viewing the T-S diagrams which have been clustered into three different types, typical examples are shown in Figures 5 to 7. Figure 8 plots the different T-S types on the glider routes. Figure 5 shows that the water column was generally well mixed in the bathymetry range of 0–20 m and in deeper water during the start of glider "k89" transit when it was between 22.5°S and 22.55°S. Generally, as the water depth increased the T-S diagram showed a greater range of temperature and salinity values and the resulting plot varied from a curve as shown in Figure 6 to a rotated L or hook shape over a small temperature and salinity range. In the 41-60m water depth the T-S data often included a hysteresis as shown in Figure 7 which is a 3D temperature salinity depth diagram. The data in this figure shows that the T-S hysteresis is due to the salinity measurements. There are two possible causes for the hysteresis: firstly, it may be due to

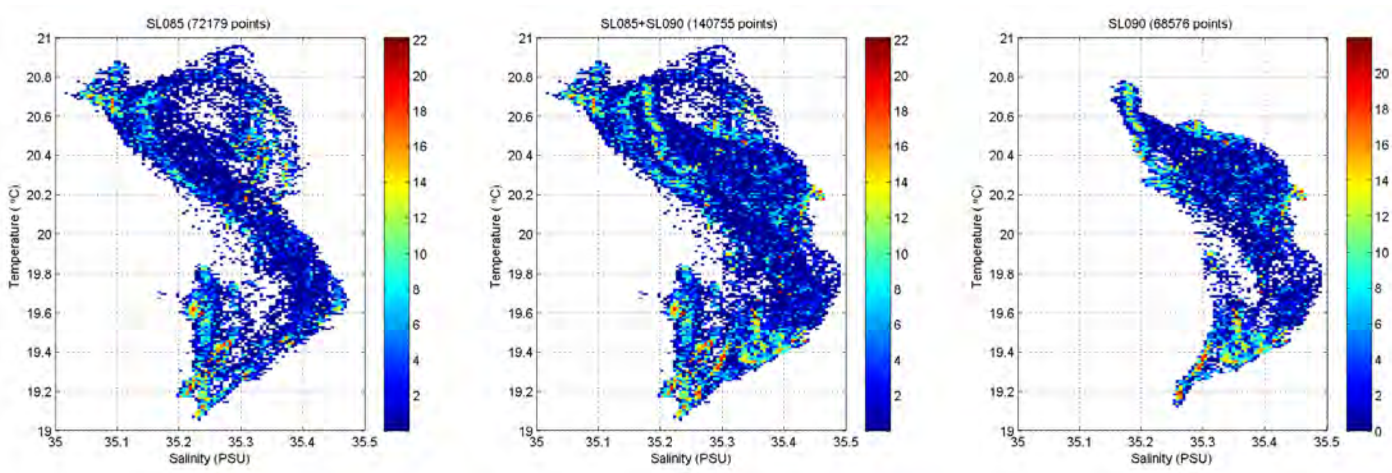


Figure 3. Temperature Salinity diagram for the two gliders. The colour intensity scale shows the number of points which recorded each temperature salinity pair

different sensor measurement latency times during the downcast/ upcast cycle or secondly, it may reflect an actual water column event. There are no independent measurements to clarify this. If the cause is due to a latency issue then either a correction needs to be applied to the salinity measurement or some of the data is excluded in the speed of sound calculation.

**Tidal Analysis**

This area of the Great Barrier Reef is noted for its macro tidal ranges [7]. Table 1 shows the tidal information for 3 days of the trial. During the time of the significant change in the T-S plots, the night of Thursday 14th and Friday 15th morning the tidal heights were at a maximum due to the new moon as indicated by the open circle next to the “Friday 15” caption.

Middleton [10] notes that the surface temperature increases from the coast across the shelf and the salinity decreases across the shelf. This is in agreement with the data presented in Figure 9. Both of these findings are supported by the data for the eastward leg from location 22.55°S 150.9°E where the maximum surface temperature was 20.1°C with a steady increase until 22.5°S 151.1°E where the maximum surface temperature was 20.8°C. After this time, the glider apparently moved away from the cool water jet and the maximum surface temperature remained stable down to location 22.6°S 151°E.

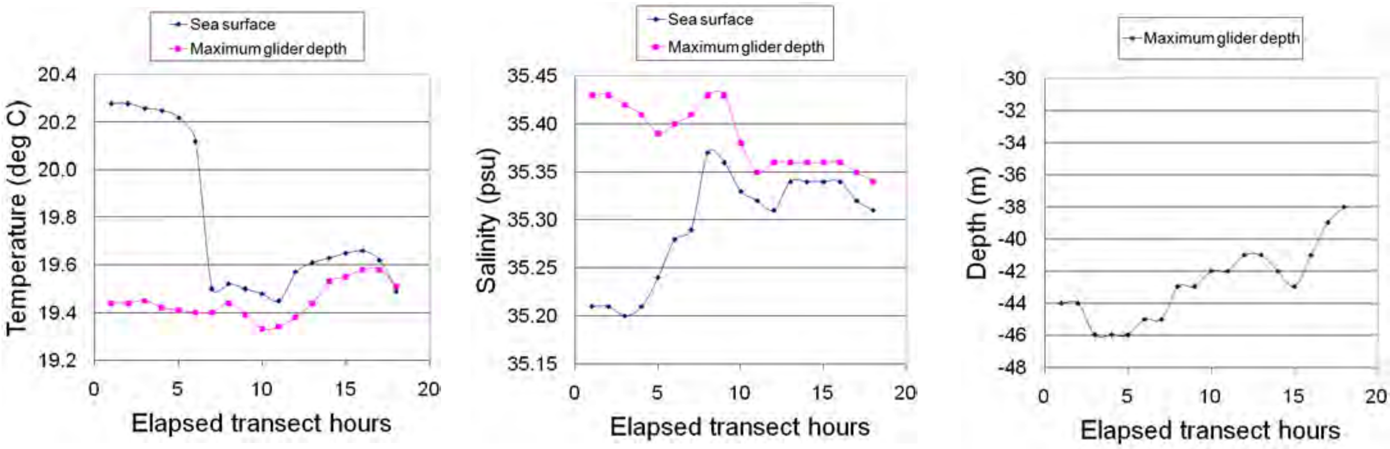


Figure 4. Temperature, salinity and maximum glider depth during a 20 hour transit time for glider “k90”

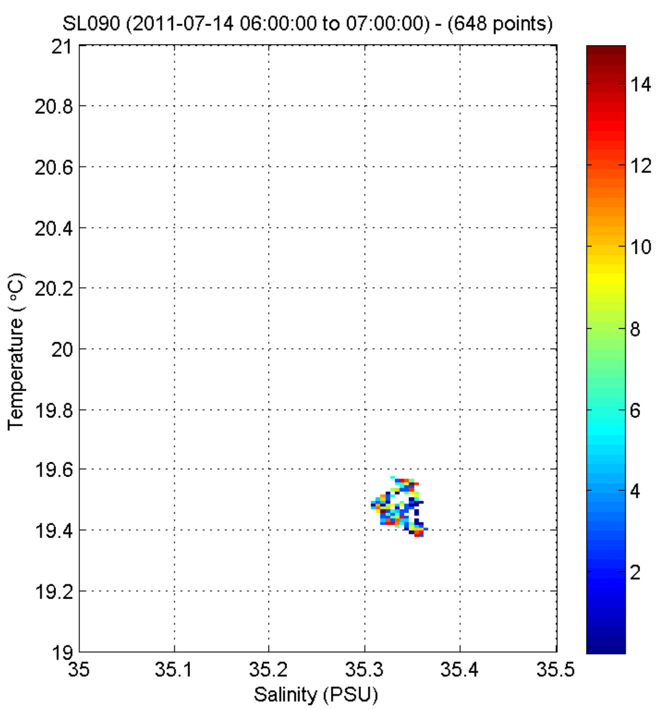


Figure 5. T-S diagram of well mixed water based on 1 hour of data. The colour intensity scale shows the number of points which recorded each temperature salinity pair

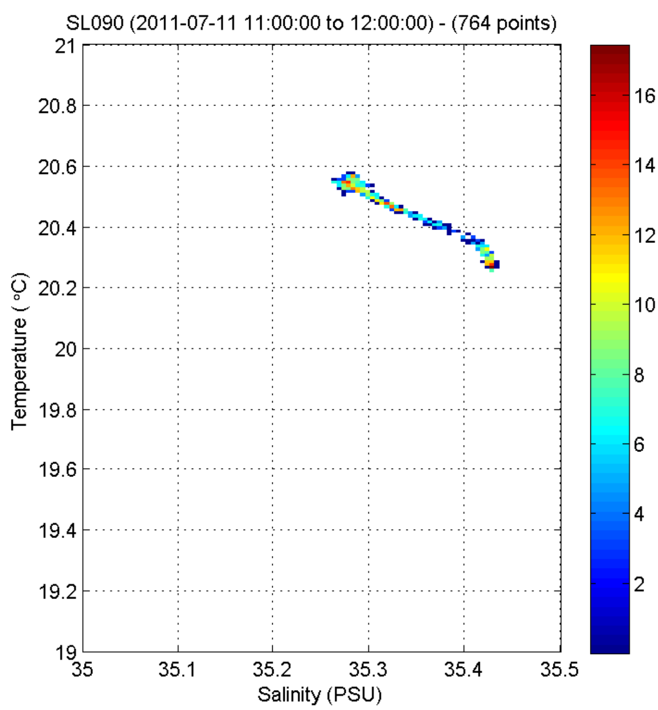


Figure 6. T-S diagram for water column with a vertical gradient in properties based on 1 hour of data. The colour intensity scale shows the number of points which recorded each temperature salinity pair. Water depth is 50 metres

Table 1. Local tidal information. Height is in metres (extracted from [8])

**Port Alma - Times and Heights of High and Low Waters**
**July - 2011**

(Peaked Island, add 3 minutes for approximate tide times)

| Wednesday 13 | | Thursday 14 | | Friday 15 | |
|---|---|---|---|---|---|
| Time | Height | Time | Height | Time | Height |
| 0209 | 0.98 | 0255 | 0.87 | 0336 | 0.82 |
| 0744 | 4.19 | 0829 | 4.27 | 0909 | 4.32 |
| 1408 | 0.87 | 1451 | 0.81 | 1529 | 0.80 |
| 2027 | 5.25 | 2107 | 5.29 | 2143 | 5.26 |

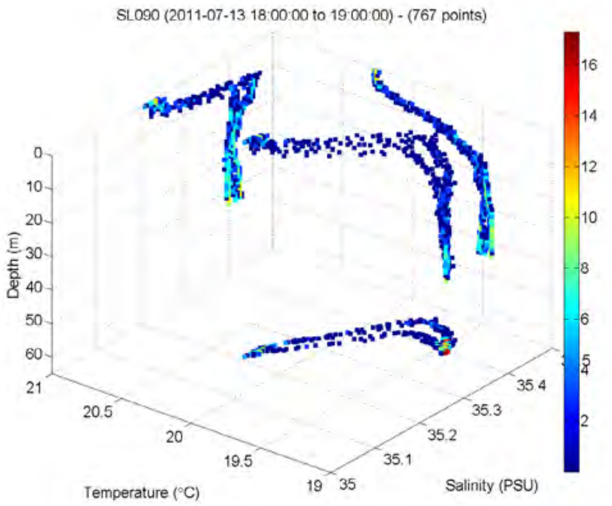


Figure 7. 3D Temperature Salinity Water Depth diagram for 1 hour of data which displayed hysteresis. The colour intensity scale shows the number of points which recorded each temperature salinity pair

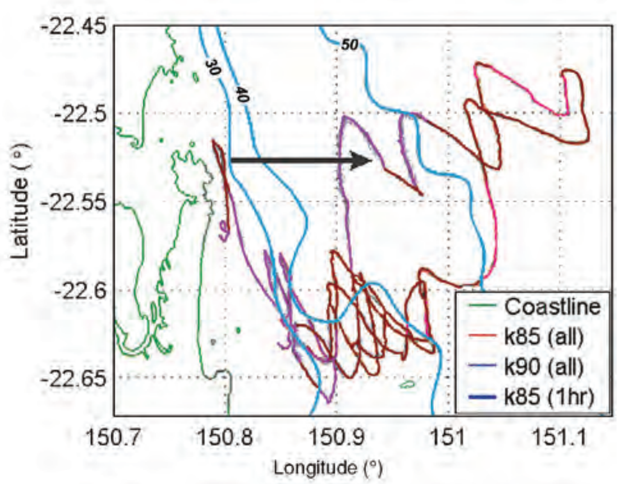


Figure 8. Cluster analysis of the T-S data based on 1 hour sampling. The arrows indicate the reported current flow. The purple overlay of the routes indicate the possible southern edge of a cold water jet and is based on T-S diagrams which are similar to Figure 5. The brown route overlay is for locations where the T-S diagram is similar to Figure 6. The pink route overlay is for locations where the T-S diagram is similar to Figure 7

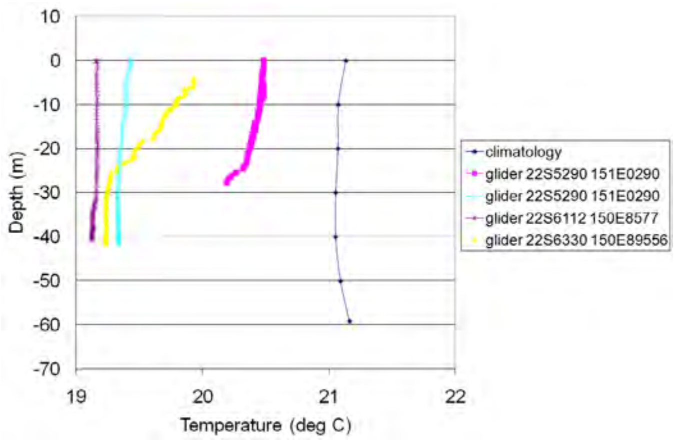


Figure 9. Comparison between the temperature profiles recorded at different glider locations against climatology database [9]

**Consecutive glider up and down casts**

A 7.5 km northerly route starting from approximately 150.9°E 22.6°S and ending at approximately 150.9°E 22.5°S was chosen (see Figure 8). The T-S characteristics of this route are of well mixed water similar to those given in Figure 5. Figures 10 and 11 show the raw temperature and salinity concatenated, contiguous, upcasts profiles as a function of depth. The average distance travelled and the elapsed time from the start of the route for each upcast is given in Figure 12. The jump in distance between cycle 5 and 6 in Figure 12 is assumed to be due to a GPS adjustment and the range along the route would need to be reduced accordingly.

Although the temperature and salinity ranges are small for each of the plots, there is evidence of the dynamics of the water column present in Figures 10 and 11. For example, there is a parcel of warm water present near the surface in Figure 10 from cycle 6-8. The salinity plot (Figure 11) shows an evolution from slight stratification at cycle 1 to well mixed from cycle 9 onwards.

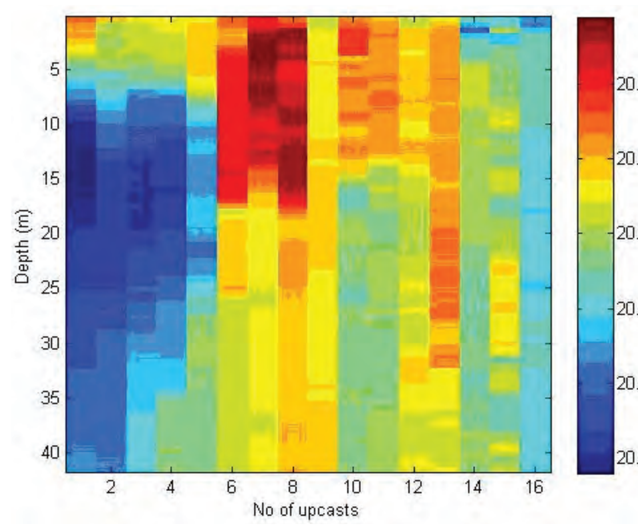


Figure 10. Sequence of contiguous upcast temperature profiles (°C) as a function of depth

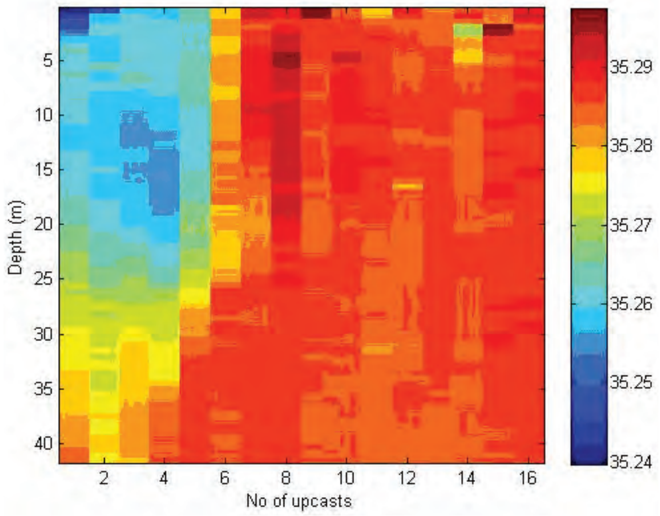


Figure 11. Sequence of contiguous upcast salinity profiles (psu) as a function of depth

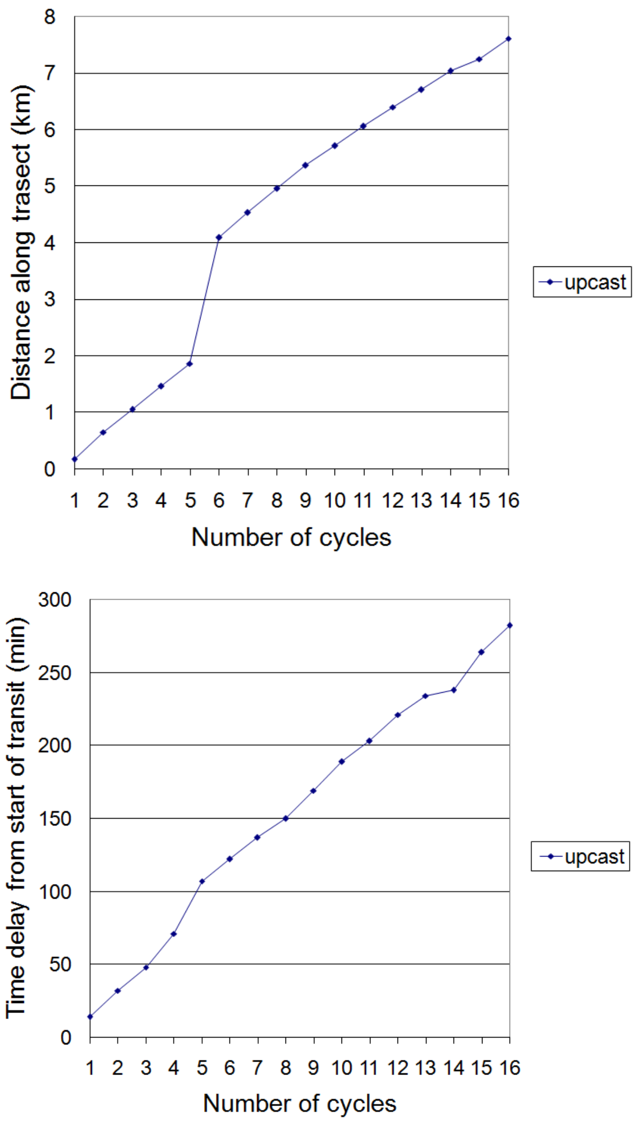


Figure 12. Distance and time delay along upcast route

The temperature and salinity profiles have been converted into sound speed profiles for five ranges from the start of the transect as indicated in Figure 13. Although, the temperature and salinity ranges for this route are small, the resulting sound velocity profiles are noticeably different, particularly in the first 5 to 10 metres. As the glider moved along the route, for a 3 hour period and 2 km distance, the sound velocity profile became primarily dependent on depth due to the well mixed water for the entire water column. The mechanism for the mixing could be tidal or due to the Clinton Cape jet or both. Measurements across at least two tidal cycles along the same track would assist in assessing the relative contribution of each mixing mechanism.

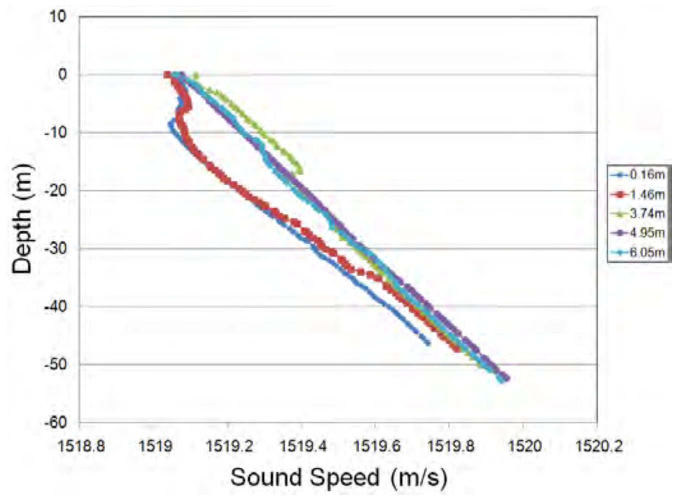


Figure 13. Sound speed profiles based on concatenated upcast glider measurements using the raw ranges given in Figure 11

Figure 14 shows the full sequence of contiguous sound speed profiles using the salinity and temperature data for the full water depth given in Figures 10 and 11. The profiles show the upward refracting sound velocity profiles are a constant feature of the track with some small variations near the surface. Figure 15 shows sound velocity profiles at an easterly point in the route.

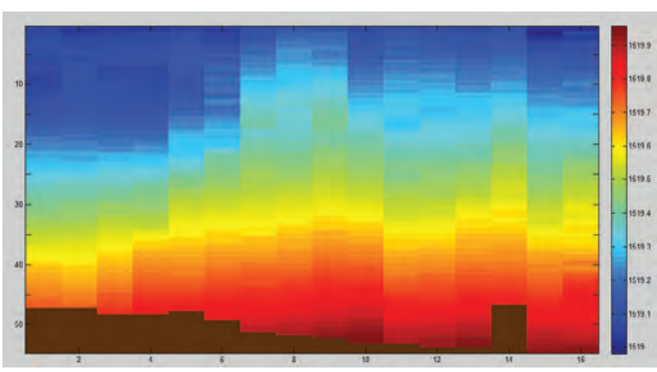

Figure 14. Sound speed profiles based on concatenated upcast glider measurements using the raw ranges given in Figure 12

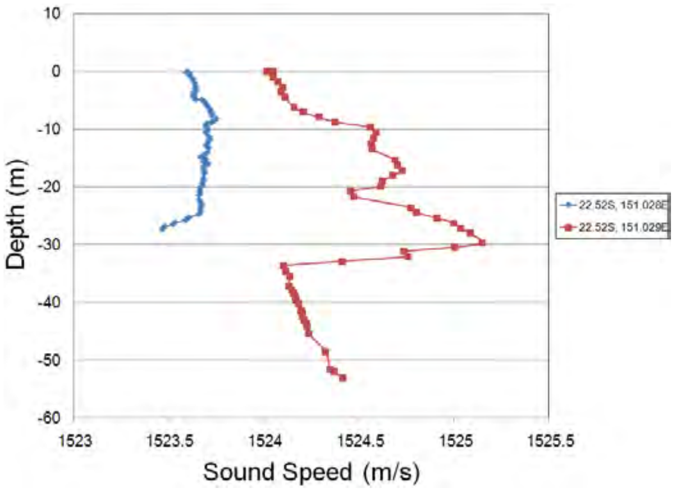


Figure 15. Up cast sound speed profiles at an easterly point of the route

## DISCUSSION

The goal of this preliminary study was to look at the suitability of glider data as an input for nowcast range dependent acoustic transmission loss calculations. The conclusion reached based on the dynamic datasets reviewed is that if one uses this data directly to calculate sound speed profiles then a number of caveats would need to be applied. In the first instance there is the issue of the salinity hysteresis to be resolved. In the second instance, the profiles need to be aligned in time for the different upcast/downcast time delays noting that the data has the finest time resolution in depth compared to the coarser and variable time resolution in range. In the third instance, the location of the measurement may require a correction due to GPS adjustments. Finally, there is the need to include the differences between individual upcast/downcast. A solution to the latter issue is to separate the data into two sets or to average the upcasts and downcasts. One set would consist of upcasts and the other down casts. These could each be used to predict the transmission loss and detection range. This may result in different detection ranges being calculated and the concept of "range of ranges" (i.e. a number of possible ranges based on the dynamics of the water column) needs to be invoked for the detection range calculations.

Rather than directly using the glider data after applying suitable corrections, a more preferred approach is to use it in conjunction with a priori knowledge or as an input into a local regional oceanographic model. As indicated in this study, the general location of oceanographic features, such as the northward moving boundary current and the Cape Clinton jet can be given as existing knowledge. The role of the glider data could be to refine this information for nowcast predictions. In particular, the glider data can be used to infer greater detail, such as steric height (steric height anomaly is the difference between the height of a given water column and the height of an ideal 0°C, 35 psu salinity column,), which could supplement existing satellite observations. The given set of glider data has a limited lifetime which can be extended with the inclusion of an afternoon effect model (which calculates the effect of the warming of the top of the ocean), but at the expense of requiring a number of additional inputs such as wet and dry air temperature. The use of the afternoon effect model can also allow the glider data to be aligned to a particular instant in time. The concept of "range of ranges" is also suitable in this context as a means of including the variability of the measured parameters in the range prediction result.

## ACKNOWLEDGEMENTS

The author wishes to thank Dr Adrian Jones of DSTO for organising and providing the glider data and Andrew Pidgeon of Thales for his assistance in the production of some of the figures in this paper.

## REFERENCES

[1] A.D. Jones, J.S. Sendt, Z. Yong Zhang, P.A. Clarke and J.R. Exelby, "Optimisation of transmission predictions for a sonar performance model for shallow oceans regions", *Proceedings of Acoustics 2002*, Adelaide, Australia, 13-15 November 2002
[2] A.D Jones, J.S. Sendt, Z. Yong Zhang, P.A. Clarke and A. Maggi, "Modelling the acoustic reflection loss at the rough ocean surface", *Proceedings of Acoustics 2009*, Adelaide, Australia, 23-25 November 2009
[3] BLUElink ocean forecasting for Australia's future, http://www.csiro.au/en/Organisation-Structure/Flagships/Wealth-from-Oceans-Flagship/BLUElink-Brochure.aspx (last accessed 20 March 2013)
[4] P.N. Jackson and A.D. Jones, "Slocum gliders deployed by the Defence Science and Technology Organisation (DSTO) in the Coral Sea in July 2011 (DSTO_T11_20110711 and DSTO_MadmaxTest2011_20110711)", Defence Science and Technology Organisation (DSTO), 2012
[5] D.M. Burrage, C.R. Steinberg, W.J. Skirving and J.A. Kleypas, "Mesoscale circulation features of the Great Barrier Reef region inferred from NOAA satellite imagery", *Remote Sensing of Environment* **56**, 21-41 (1996)
[6] J.A. Kleypas and D.M .Burrage, "Satellite observations of circulation in the southern Great Barrier Reef, Australia", *International Journal of Remote Sensing* **15**, 2051-63 (1994)
[7] The Tides of Australia, *www.abs.gov.au › ABS Home › Statistics*
[8] Bureau of Meteorology, Tide Predictions for Queensland, http://www.bom.gov.au/oceanography/tides/MAPS/gbr.shtml#map (last accessed 20 March 2013)
[9] CSIRO Atlas of Regional Seas (CARS 2000), www.marine.csiro.au/~dunn/eez_data/atlas.html (last accessed 20 March 2013)
[10] J.H. Middleton, P. Coutis, D.A. Griffin, A. Macks, A. McTaggart, M.A. Merrified and G.J. Nippard, "Circulation and water mass characteristics of the southern Great Barrier Reef", *Australian Journal of Marine Freshwater Research* **45**, 1-18 (1994)